ESD-TR-71-141

Technical Note

1971-29

S. L. Zolnay

An Acquisition and Tracking Receiver for Satellite-to-Satellite Relaying at 55 GHz

11 May 1971

Prepared under Electronic Systems Division Contract F19628-70-C-0230 by

Lincoln Laboratory
MASSACHUSETTS INSTITUTE OF TECHNOLOGY
Lexington, Massachusetts

Approved for public release; distribution unlimited.

MASSACHUSETTS INSTITUTE OF TECHNOLOGY

LINCOLN LABORATORY

AN ACQUISITION AND TRACKING RECEIVER FOR SATELLITE-TO-SATELLITE RELAYING AT 55 GHz

S. L. ZOLNAY

Group 63

TECHNICAL NOTE 1971-29

11 MAY 1971

LEXINGTON MASSACHUSETTS

The work reported in this document was performed at Lincoln Laboratory, a center for research operated by Massachusetts Institute of Technology, with the support of the Department of the Air Force under Contract F19628-70-C-0230.

ABSTRACT

This note deals with the design of an acquisition and tracking system for inter-satellite communication. The problems of acquisition and tracking of position and of frequency are addressed. These are defined for the planned LES-8 and -9 satellites and a system design is proposed. The anticipated performance of the system is evaluated.

Accepted for the Air Force
Joseph R. Waterman, Lt. Col., USAF
Chief, Lincoln Laboratory Project Office

I. INTRODUCTION

The purpose of this Technical Note is to discuss some of the important technical issues related to the acquisition and tracking of EHF cross-links with immediate applications to the LES-8 and -9 satellites and with possible extensions to other similar communication systems planned in the future.

EHF crosslinks are characterized by narrow beam antennas even with modest size apertures. This requires the alignment of the boresight axes of the antennas along the line of sight between the two spacecraft and the maintaining of this alignment between the antennas. Additionally, at the extra high frequency of the carrier, the relative satellite velocities cause Doppler shifts, and oscillator instabilities produce an offset of the carrier. Acquisition then consists of scanning the spatial uncertainty of the target location while simultaneously resolving the frequency uncertainty in the signal. When this is successfully achieved, namely when the target is in the beam and the carrier frequency is centered in the bandwidth, then the tracking of the various parameters can be initiated and cross-link communication commences.

Unless the spatial and frequency uncertainties are less than about one half-power beamwidth and one bandwidth respectively, the antenna should be scanned in position and the local oscillator swept in frequency. If these uncertainties are much greater than one beamwidth and one bandwidth, then it may be desirable to augment scan capability with a search strategy. In case of possible malfunctions which may occur during launch or because of differential perturbation of orbit parameters, it may be necessary to have such a strategy in order to acquire. During acquisiton the signal must be detected. This is a statistical process which requires the evaluation of the detection probability as a function of signal-to-noise ratio and of threshold setting and the evaluation of the false alarm probability as a function of threshold level. Finally, it is helpful to know in advance where to begin looking for the target and it also helps to know the order of magnitude of the parameters one expects to find as well as their variations as functionsof real time.

Thus, this note deals with some of the results of orbital studies, orbital and cross-link parameters, their variations and their effects upon acquisition and tracking system design. In particular we consider questions of search and scan, detection probabilities, false alarm rates, bandwidth requirements, sweep rates, threshold setting, acquisition procedure, and tracking system. The conceptual block diagram of a candidate acquisition and tracking receiver is proposed and its expected performance in terms of tracking accuracy and in terms of its effect upon the communication system is evaluated.

II. LINK PARAMETERS

A study of various orbits was carried out to aid in problem definition, system selection, design and analysis, and for the specific purpose of pre-computing the link parameters and their variations with time. The link parameters of interest are range, doppler and look angles from one satellite to the other and the time rate of changes of these same parameters. LES-8 and -9 are planned to be launched into an Earth-synchronous, circular orbit coincident with the plane of the equator. The satellites, after separation from the rocket, will drift apart and after a few months will reach their stations which will be separated by a central angle of 90°. If the launch and stationkeeping go as planned, the acquisition and tracking problems will be minimal: the link parameters between two relatively stationary satellites in identical, circular orbits are invariant. If, however, the resultant orbits should have some small eccentricity or differential inclination, a varying component will be superimposed upon the steady state values of the link parameters. For the purposes here we assumed certain orbital parameters and computed the crosslink parameters and their variations. The results are shown in Table I together with the assumed values for the orbital parameters. The periods of the varying components are seen to be very long; they are in fact the orbital periods of the satellites. The amplitudes are reasonably small: they are directly proportional to the magnitude of eccentricity for small values of this parameter. An increase in eccentricity by a factor of ten would cause a proportionate increase in the amplitudes. Changing the separation between the satellites to 120° would increase the range to 75,000 km and reduce the average value of the pitch

TABLE I

VARIATIONS IN CROSSLINK PARAMETERS

Range, km	$61{,}000 + 400 \sin 2\pi t/24$
Range Rate, km/hr	$100 \cos 2\pi t/24$
Peak $\dot{R}$, km/sec	0.03
Doppler, kHz @ 55 GHz	$5 \cos 2\pi t/24$
Doppler Rate, kHz/hr	$- 1.3 \sin 2\pi t/24$
Peak Doppler Rate, Hz/sec	0.36
Pitch, deg	$45 + 1 \sin 2\pi t/24$
Pitch Rate, deg/hr	$0.3 \cos 2\pi t/24$
Roll, deg	0

Assumed Orbital Parameters:

Semi-major axis:	6.6 earth radii
Inclination to plane of equator:	0°
R.A. of ascending node:	310°E
Argument of perigee:	270°
Separation between satellites:	90°
Eccentricity	0.01

to 30°. A differential inclination between the planes of orbits of the satellites--an unlikely occurrence since they will be launched by the same rocket--could also cause variations in cross-link parameters. In this case the periods of the varying components would be one half of the orbital period and the amplitudes would be proportional to the magnitude of the differential inclination. To produce variations in the link parameters of similar amplitude to those listed in Table I, a $\Delta I = 10^{\circ}$ is necessary, which would also cause sinusoidal variations in roll of 6° amplitude but with a period equal to the orbital period.

Let us next compute the P_r/No value for the EHF crosslink. We assume an operational frequency of 55 GHz, parabolic dishes of 18" diameter and 55% aperture efficiency, antenna noise temperature of $100^{\circ}K$, $290^{\circ}K$ ambient temperature, and a system noise figure of 9.5 db. The output of the solid state transmitter is modestly assumed at ¼ watt, the guide losses are taken to be 1 db each, and the separation between the satellites is 60,000 km. A 2 db margin for errors is included in the computation.

$$\frac{P_r}{No}\ (\text{db-Hz}) = -10 \log_{10} k - 10 \log_{10} \left[\alpha T_{ant} + T_{amb} (1 - \alpha) + T_{amb} (NF - 1) + \sum_{m=2} \frac{T_m}{g_{m-1}} \right] + P_o + G_T + G_R - P_L - L_G - M(e)$$

$$\frac{P_r}{No}\ (\text{db-Hz}) = 228.6 - 10 \log_{10} \left[.795 \times 100 + 290\ (.205) + 290\ (8.9 - 1) + 0 \right] - 6 + 45.8 + 45.8 - 222.8 - 2 - 2$$

$$= 53.6$$

where k is Boltzman's constant, P_o is output power, G is antenna gain, P_L is path loss, L_G is guide losses, M(e) is error margin, and the expression in the brackets is system noise temperature referred to the input of the first stage. With the above assumptions the computed P_r/No value on the EHF crosslink is 53.6 db-Hz. We postulate a binary phase-shift keying and a bit error rate $P_b \leq 10^{-5}$. This will require an $E_b/No = 9.7$ db. For a 10 kilobits per second data rate the margin, or excess capacity, is 3.9 db.

III. ACQUISITION

A. Position Scan

To augment scan capability and to acquire in case of launch malfunctions or orbital degradations, the general problem of search has been considered. Search has been found to be a secondary requirement, necessary only in case the position and frequency uncertainties exceed planned scan and sweep capabilities. This is not a likely occurrence even in case of moderately elliptic orbits. On the basis of practical experience with previous satellites it can be anticipated that the uncertainty in target position will be on the order of one beamwidth (about 1°). The pre-computed value of Doppler shift from Table I is on the order of the bandwidth required to accommodate the postulated data rate. Thus, unlimited search in position and frequency is not planned. However, it is desirable to consider the problems of scanning in position and sweeping in frequency. The subject of these considerations is a simple method of probing over the extents of the uncertainties in three coordinates--pitch, roll, and frequency for the purpose of acquiring the position and frequency of the target. The availability of such a scheme also tends to relieve the stability and accuracy requirements.

The acquisition problem is sketched in Fig. 1. Look angle uncertainties are shown in terms of the half-power beamwidths of the antennas, frequency uncertainty in terms of the bandwidth. Due to the narrow antenna beams, maximum power for crosslink communication is achieved only when the boresights are collinear (indicated by the dashed line in Fig. 1). To bring this condition about, both antennas must scan, one scans much slower than the other. While the fast scanning beam completes the scanning of the entire NXM frame, the slow scanning beam remains in the same spot. The length of time for the fast

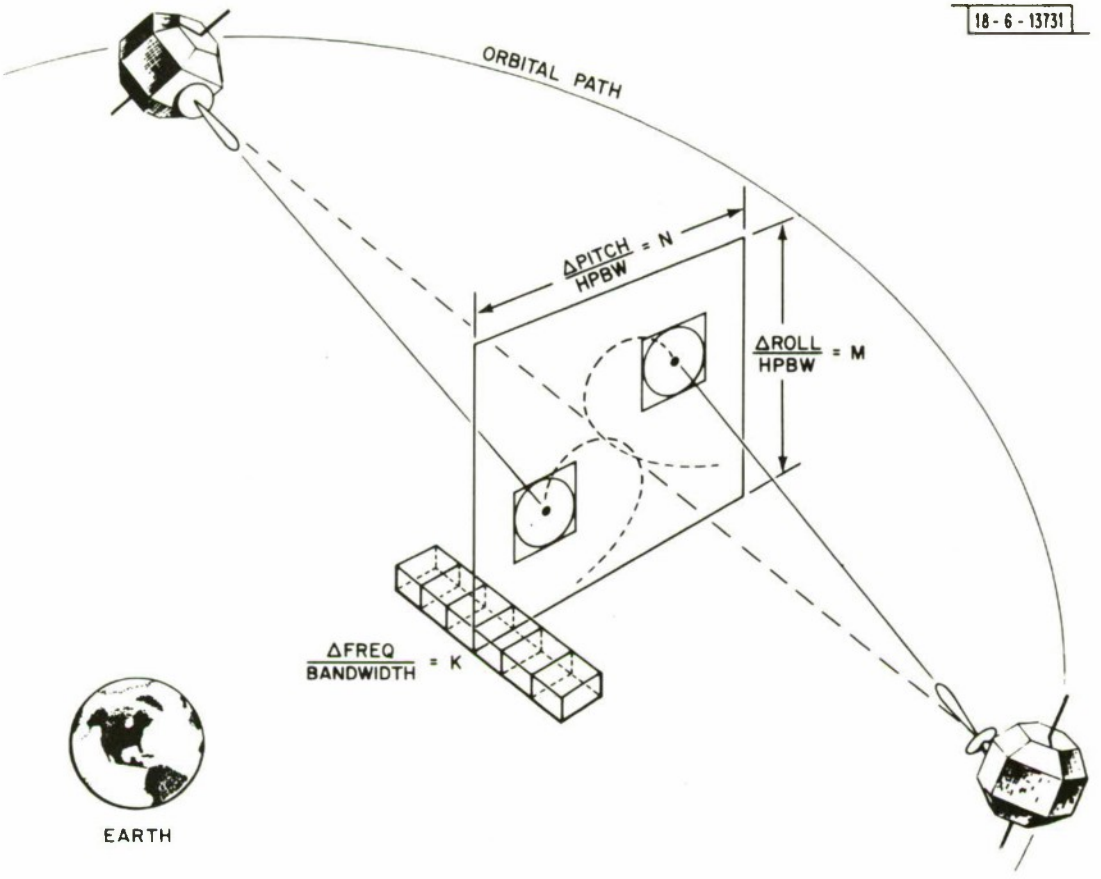

Fig. 1. The position scan and frequency sweep problem for acquisition.

scanning beam to remain in one spatial resolution cell depends on the one hand on how fast the beam can be steered mechanically (or electronically), and on the other hand on the ratio of frequency uncertainty to the square of the bandwidth, since the rise time of a pulse in a bandwidth B is inversely proportional to B. The maximum acquisition-time in case of large frequency uncertainty narrow bandwidth and rapid beam scanning is

$$\text{Acquisition time (max)} \propto (\text{NXM})^2 \frac{\Delta f}{B^2}$$

If the frequency sweep can be accomplished during the time the antenna beam dwells in one spot, then the maximum acquisition time is governed by the mechanical scan rate:

$$\text{Acquisition time (max)} \propto \frac{(\text{NXM})^2}{\text{scan rate}}$$

For our purposes, the latter situation is of interest. One of the satellite antenna beams will be caused to scan as fast as mechanically acceptable: about 1°/sec. This choice and the magnitude of the position uncertainty determines the acquisition time; it will also set an upper limit on the time for frequency acquisition which in turn will influence the sweep rate and the magnitude of the frequency uncertainty that can be searched in this time limit at the prevailing signal levels.

For the purpose of defining the problem, we assume that it will be possible to aim the narrow beam antenna from either satellite toward the other along the line of sight with an error not exceeding $\pm 0.5^{\circ}$ per coordinate axis. This figure is based on the best currently available estimates and includes the effects of imperfect stationkeeping and of less than ideal orbital parameters. For the sake of being conservative, the 0.5° is regarded as one standard deviation, and thus the three sigma limit of pointing accuracy is $\pm 1.5^{\circ}$. The antenna half-power beamwidths are 0.8°, the 1.5° figure represents $\pm$ 2 HPBW's, and the extent of the position uncertainty to be scanned is 4 x 4 HPBW's. We would expect that the probability is at least 99% that

the line of sight is within this region. Making the fast scanning antenna move at the rate of 0.8^{o}/sec = 1 HPBW/sec and making the scan pattern such that the individual scans overlap at the - 3 db points, the maximum acquisition time is $(4 \times 4)^2 = 256$ seconds or about 4 minutes. On the average the antenna beam dwells in one spatial resolution cell for 0.8 second.

The choice of making the scan pattern overlap at the - 3 db point follows from the consideration that if the target is detected within the half-power beamwidth the position tracking system will cause the boresight to align itself promptly and unambiguously with the line of sight to the target; i.e., the antenna will "pull-in". The above scan pattern is conservative, the antenna would pull into position eventually as long as the target was detected within less than about one beamwidth from the boresight. The choice in scanning overlap leads to considering the minimum signal level during acquisition and the setting of the threshold level. We would like to stop the position scan when the antennas are within their - 3 db beamwidths to the line of sight. In the process of stopping, the antennas coast for not more than $1/10^{o}$ which can represent an additional power level reduction of approximately 2 db per antenna under the worst set of circumstances. Thus the minimum signal level during acquisition is - 10 db relative to the level of maximum P_r. This is the signal level we will use in considering the maximum sweep rate and largest frequency uncertainty to be searched; we also choose this level in setting the level of the threshold device. Setting the threshold at this level could lead to the undesirable situation that the scanning stops when the antennas are slightly more than the HPBW from the line of sight and the received power level drops below the minimum. Two events are likely in this case of triggering at the threshold. The threshold device "unlocks" due to the reduced power level and the sweep and scan are resumed. Since the scan is in terms of HPBW, either the next or some future scan will be within a closer range of the line of sight resulting in detection well above threshold. The second likely event is that the threshold device holds because the received power level is only slightly reduced from the design choice. In this case we are well within pull-in range.

B. Frequency Sweep

The sources of frequency uncertainties on the EHF crosslink are threefold: instabilities in the transmitter oscillator, instabilities in the receiver local oscillator, and Doppler shift due to the motion of one satellite relative to the other. The Doppler shift at 55 GHz carrier from Table I is 5 kHz. The current best estimate of the oscillator instabilities in each of the satellites is 4×10^{-8} which includes 1 part in 10^8 for variation with temperature and 3 parts in 10^8 for aging. For the chosen carrier frequency these values translate to a 2.2 kHz uncertainty, thus the total frequency uncertainty is $\pm$ 7.2 kHz. On the basis of this estimate we round off and assume a frequency uncertainty of $\pm$ 10 kHz and evaluate system performance and requirements using this figure as a benchmark. For the postulated data rate of 10 Kbps and binary-PSK modulation the bandwidth of a filter matched to one bit is 20 kHz. Since the assumed uncertainty places the carrier at the edge of the bandwidth, it will be necessary to acquire and track the incoming signal. Because of the modulation format it will be necessary to reconstruct the carrier in the receiver. The solutions to this specific problem of acquiring a reconstructed carrier from a bi-phase modulated signal by linearly sweeping the frequency of the local oscillator and monitoring the output of a narrow band energy detector have been worked out in detail[1,2]. The situation for the LES-8, -9 satellites is essentially the same as that considered in Refs. 1 and 2. In this note we are primarily concerned with position tracking, for sake of completeness we address the entire problem of acquisition and tracking of frequency and phase, and of position. The salient results of Refs. 1 and 2 are included partly here and mostly in the Appendix with the gracious permission of the authors. These are appropriately modified and adapted to the LES-8 and -9 system parameters and requirements.

The conceptual block diagram of the frequency search and acquisition scheme is shown in Fig. 2. The bandpass filter, matched to one bit, and the squarer reconstruct the incoming carrier frequency from the bi-phase modulated signal. The frequency and phase of the voltage controlled crystal oscillator is caused to track the variations in the incoming carrier by the action of the phase-lock loop which of necessity operates at $2\omega_o$. By operating a phase

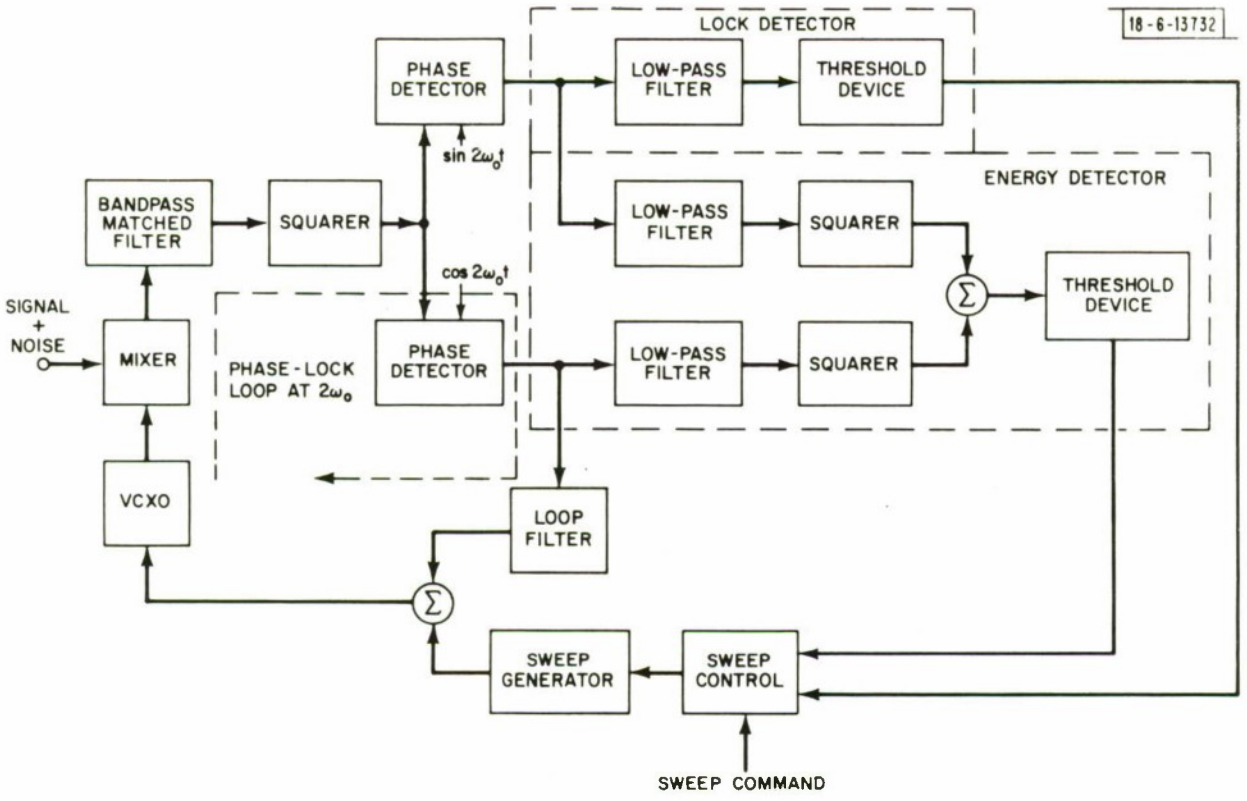

Fig. 2. Conceptual diagram of phase-lock loop with energy and lock detectors (Ref. 2).

detector in quadrature with the phase of the reference oscillator and following its output with a low-pass filter and threshold detector the presence of phase-locked conditions can be ascertained. The phase-lock loop is a nulling arrangement, the quadrature detector output, however, is maximum and proportional to carrier amplitude when the loop is locked. The outputs of both the in-phase and quadrature detectors operate into the low pass filters and squarers which together with the threshold device comprise the energy detector. The VCXO is swept in frequency by actuating the sweep generator either through the sweep command or automatically, due to the output of the energy detector and/or due to the lock detector not triggering the threshold device. The sweep generator is stopped either by the sweep command or by the presence of a threshold signal from the energy detector.

IV. POSITION TRACKING

To establish EHF crosslink communication, acquisition of position and of frequency are necessary. Once the target is acquired, the alignment of the antenna beams along the line of sight must be maintained and the carriers must be kept centered within the bandwidths. Accurate tracking insures crosslink communication, it also yields an independent set of angle sensor data the availability of which may be of considerable importance. The methods of angle sensing customarily involve the shifting of the main lobe of the antenna sequentially as in beam switching, or continuously as in conical scan, or the formation of multiple lobes as in monopulse. The method proposed here for satellite applications is a form of beam switching where the switching is accomplished by periodically reversing the RF phase of the difference channels and adding this phase modulated difference pattern to the main beam. The result is a beam offset from the boresight and the resultant signal is an amplitude modulated one where the magnitude is proportional to the offset and the phase is determined by the direction of the offset.

An understanding of the operation of the suggested position tracker can be gained by considering the antenna voltage pattern cuts shown in Fig. 3. A reasonable representation of Pattern A with even symmetry about the

boresight, normalized to unity at boresight, is

$$\text{Pattern A} = 1 \cos^2 1.18\,\Delta$$

where $\Delta = \delta\theta/\theta_{HPBW}$ is the angular offset from on-axis in terms of the half-power beamwidth. Pattern B with odd symmetry about the boresight is represented as

$$\text{Pattern B} = k \sin 2.36\,\Delta$$

where k is a number less than one when the amplitude of Pattern B is normalized by dividing it with the peak amplitude of Pattern A. These two pattern cuts are recognized as the standard monopulse sum and difference patterns in which case the nominal value of k is $\sqrt{2}/2$. The procedure is to bi-phase modulate the difference pattern and add it to the sum pattern to produce resultant Pattern C. This resultant pattern is squinted from boresight in the direction shown for a given phase relationship between Patterns A and B. By reversing the phase of the difference pattern periodically, the resultant pattern is switched to alternate sides of the boresight in synchronism with the modulation. The procedure is like beam switching in one of the two coordinates and an amplitude modulation is produced unless the target is exactly on-axis. When the addition in phase-quadrature of the other bi-phase modulated difference channel is considered, it may be seen that the resultant pattern "steps" around the boresight axis in sequence and in four discrete steps at the modulation rate.

The essential features of the tracking system are shown in Fig. 4. The performance of this phase switching tracker was analyzed in some detail by Tourdot.[3] The problem considered in this reference is a square wave amplitude modulated sinusoidal carrier in narrow-band Gaussian noise passed through a non-linear detector. One of the principal results is the expressions found for the signal power associated with the first harmonic of modulation and for the noise power in a narrow bandwidth, Δf, around the modulation

frequency after the detector. These expressions for the half-wave square law detector case are

$$P_s = (8\,a^2/\pi^2)\,(\sigma^2)\,(P_s/P_N)^2\,\lambda^2$$

$$n_a = \frac{a^2(\sigma^2)^2}{2}\left(\frac{\Delta f}{2f_B}\right)\left[1 + 2\,(P_s/P_N)\left(1 + \lambda^2 \sum_{\substack{P=-Tf_B \\ P\ \text{odd}}}^{Tf_B} \frac{4}{\pi^2 p^2}\right)\right]$$

where a is the detector constant, σ^2 = rms input noise power, Δf = narrowest bandwidth in the system; e.g., the servo loop-bandwidth, $2f_B$ = IF bandwidth and λ is the magnitude of the error voltage (see Fig. 3). The summation in the noise expression over the odd harmonics of the modulation frequency approaches 1 for very large Tf_B products where T is the period of the RF phase reversing switch. For this analysis of the sinusoidal carrier to be valid[4] for the case of the phase-shift keyed carrier it is necessary that $Tf_B >> 1$. In the null at boresight, λ^2 approaches zero and the expression for noise simplifies

$$n_a\Big|_{\text{in null}} = \frac{a^2(\sigma^2)^2}{2}\left(\frac{\Delta f}{2f_B}\right)\left[1 + 2\,P_s/P_N\right]$$

To start the antenna to move

$$P_s = n_a\Big|_{\text{in null}}$$

$$\left(\frac{8a^2}{\pi^2}\right)(\sigma^2)^2\left(\frac{P_s}{P_N}\right)^2\lambda^2 = \frac{a^2(\sigma^2)^2}{2}\left(\frac{\Delta f}{2f_B}\right)\left(1 + 2\,\frac{P_s}{P_N}\right)$$

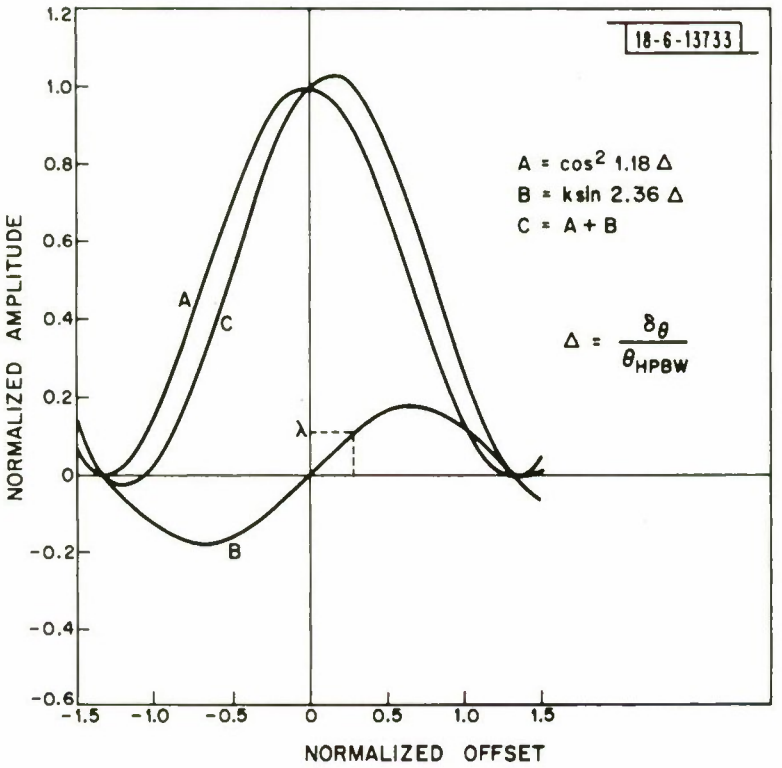

Fig. 3. Antenna voltage pattern cuts showing normalized sum, difference and resultant beams.

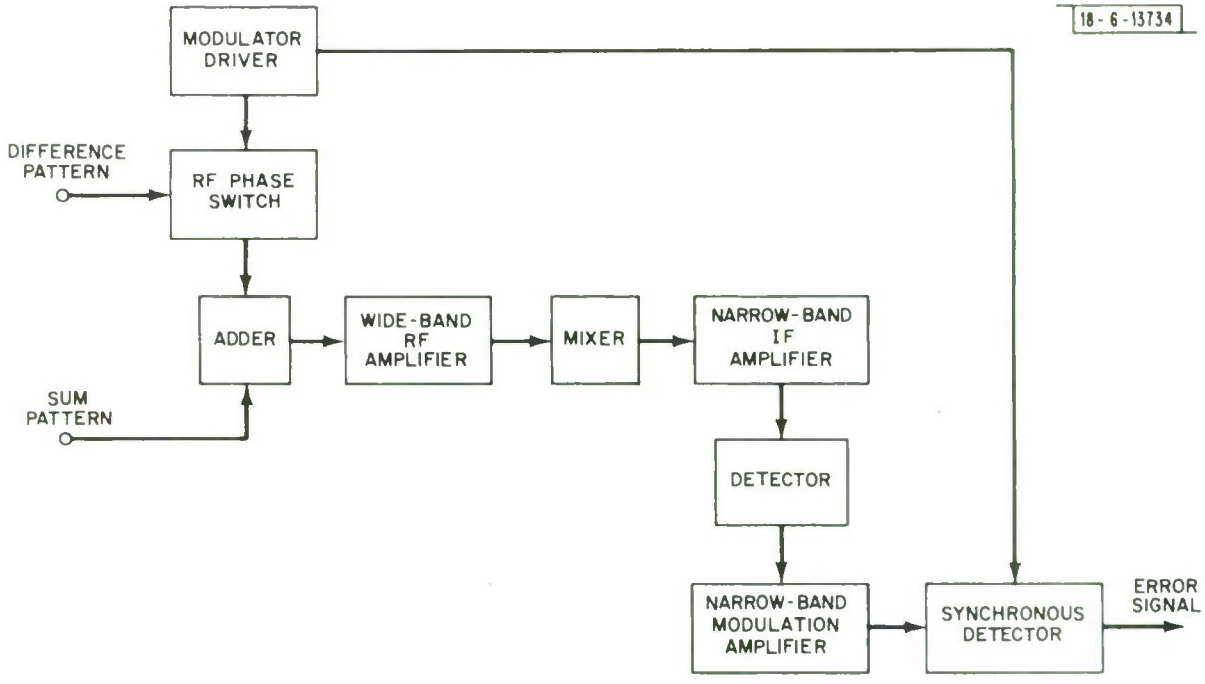

Fig. 4. Conceptual diagram of phase switching position tracker.

from which

$$\lambda^2 = \left(\frac{\pi}{4}\right)^2 \frac{1}{(P_s/P_N)^2} \frac{\Delta f}{2f_B} \left(1 + 2\frac{P_s}{P_N}\right)$$

The relationship between λ and the offset Δ from boresight is (see Fig. 3)

$$\lambda = k_m \Delta = k_m \frac{\delta_\theta}{\theta_{HPBW}}$$

where

$$k_m = \frac{\text{(error voltage)/(reference voltage)}}{\text{(angular offset)/(half-power beamwidth)}}$$

$$= \text{error slope}$$

We assume that the noise power in the null can be interpreted as an equivalent phase variance. Then

$$\sigma_\lambda^2 = \frac{\pi^2}{16} \frac{1}{(P_s/P_N)^2} \frac{\Delta f}{2f_B} (1 + 2\, P_s/P_N)$$

$$\sigma_\lambda^2 = k_m^2 \frac{\sigma_\theta^2}{\theta_{HPBW}^2}$$

Thus, the rms tracking accuracy, σ_θ, in terms of the half-power beamwidth of the antenna for the phase switching tracker is

$$\frac{\sigma_\theta}{\theta_{HPBW}} = \frac{\pi}{4} \frac{1}{k_m} \frac{\sqrt{1 + 2\, P_s/P_N}}{(P_s/P_N)\sqrt{2f_B/\Delta f}}$$

We compare this result with the maximum angular accuracy of tracking a point target with a monopulse system[5]

$$\frac{\sigma_\theta}{\theta_{HPBW}} = \frac{\sqrt{2}}{\pi}\,\frac{1}{1.02}\,\frac{1}{\sqrt{T_1 W}}\,\frac{\sqrt{1 + P_s/P_N}}{P_s/P_N}$$

where $T_1 W$ is the product of the predetection bandwidth and the post detection integration time, and uniform illumination is assumed over the aperture. A reasonable choice for the bandwidth of the position tracking servo is about 1 Hz in order to accommodate the sweep rates during acquisition and to handle sensor induced transients causing platform instabilities. The IF bandwidth for the 10 kbps data rate is at least 10 kHz, thus the IF to servo bandwidth ratio is 10^4. The above last two expressions for rms angular tracking accuracy versus P_s/P_N are shown graphically in Fig. 5 for this choice of ratio of bandwidths. The best results are achievable with a uniformly illuminated aperture. Tapering the illumination over the aperture results in reduced gain on-axis and wider beamwidth causing less accurate tracking. Practical monopulse difference patterns have error slopes of about 1.5; this is the value assumed for the curve shown for the phase switching tracker. As can be seen a phase-switching tracker based on a practical monopulse feed arrangement compares favorably with the maximum angular tracking accuracy achievable (Ref. 5). The desirable minimum tracking performance as affected by thermal noise is one-tenth of the antenna half-power beamwidth when the IF signal-to-noise power ratio is unity and the bandwidth compression factor is 10^4. It can also be seen from Fig. 5 that the phase switching tracker is predicted to achieve this accuracy per each axis at approximately P_s/P_N = -12 db. Since the anticipated signal-to-noise power ratio in the IF bandwidth is going to be about + 10 db based on bit and error rates requirements, such a tracker would have a predicted margin of at least 20 db in performance. The upper curves in Fig. 5 are also plotted for the phase switching tracker but for an error slope of 0.2 . The topmost curve is the curve directly below it multiplied by a factor of $\sqrt{2}$ to account for the rms tracking

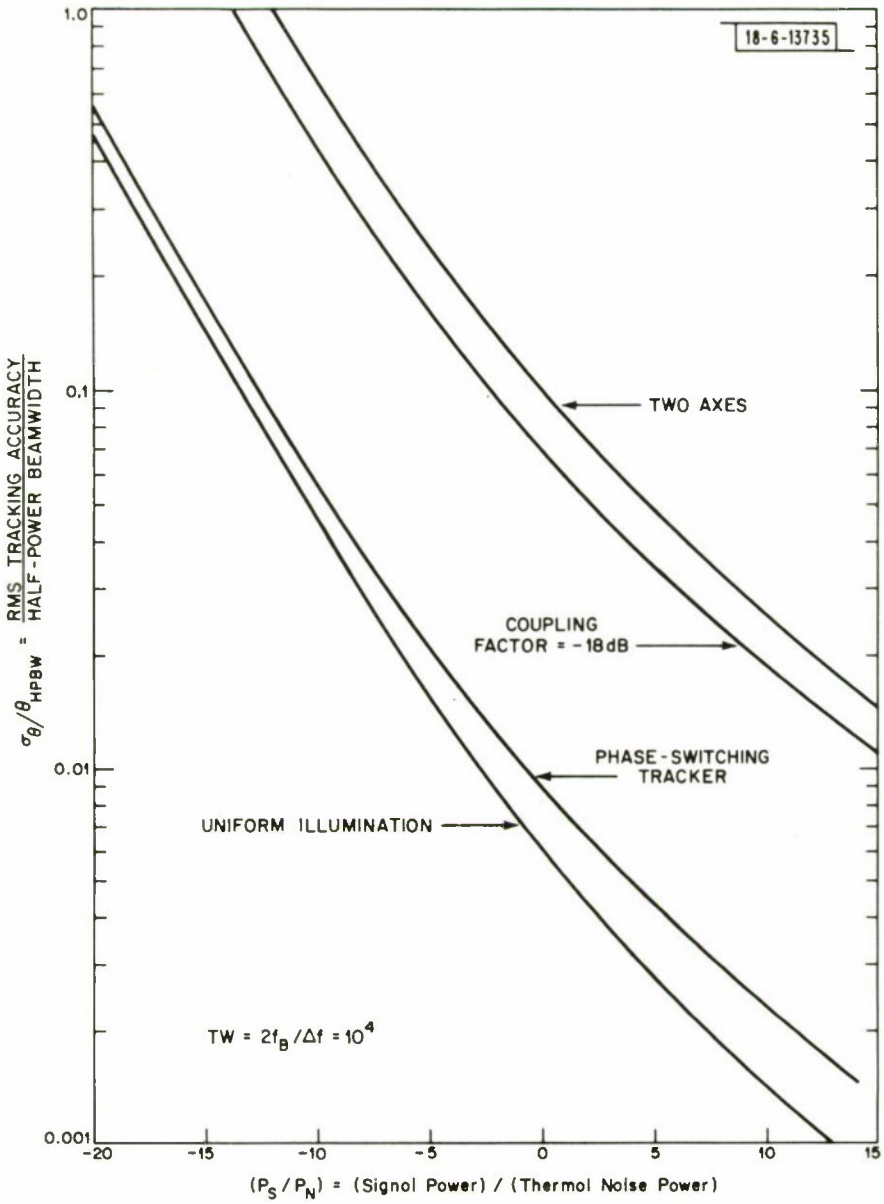

Fig. 5. Normalized angular tracking accuracy as a function of signal-to-noise power ratio.

inaccuracies occurring in each of the two axes. As can be seen, the desired tracking accuracy is predicted at the operating point when the coupling factor is - 18 db. Under coupling factor we include all losses preceding the combination of the modulated difference and sum signals; these losses are principally due to the insertion loss of the RF bi-phase modulator and the adder in Fig. 4. This allows considerable freedom in the design of the feed system and on the basis of the above considerations a feed different from the conventional monopulse is currently under consideration. Briefly, this feed will have a main horn surrounded by four auxiliary horns the outputs of which will be phase modulated and combined with the output of the main horn. The resultant beam is switched about the boresight by appropriate phasing and combining of the auxiliary outputs in a way that is similar to the process described above for the standard monopulse feed. The anticipated tracking performance for an equivalent error slope of about 0.2 should be as drawn by the topmost curve in Fig. 5. The margin in this system is about 10 db by design.

When the tracking accuracy is 0.1 x HPBW the expected loss in gain is about 0.1 db as can be seen from Fig. 6. Arbitrarily we set 1 db as the average gain loss allowable due to poor tracking performance. This occurs when the error reaches about 0.3 x HPBW. From Fig. 5 the rms tracking accuracy is of this magnitude when the P_s/P_N = - 6 db. At this point the communication channel is degraded by 16 db, that is to say in order to maintain the same bit error rate the data rate would have to be reduced by a factor of forty, or, alternately, if the design data rate is maintained, the bit error rate increases by a factor of forty. It may be said that the communication channel is seriously jeopardized at this point, whereas the expected performance in the tracking channel on the average is marginal.

V. PROPOSED SCHEME

The functional block diagram of the candidate acquisition and tracking receiver is shown in Fig. 7. Some of the features of the system are as follows. The receiver tracks on the available incoming energy where all of the power is used for data transmission and no power is wasted in a separate beacon

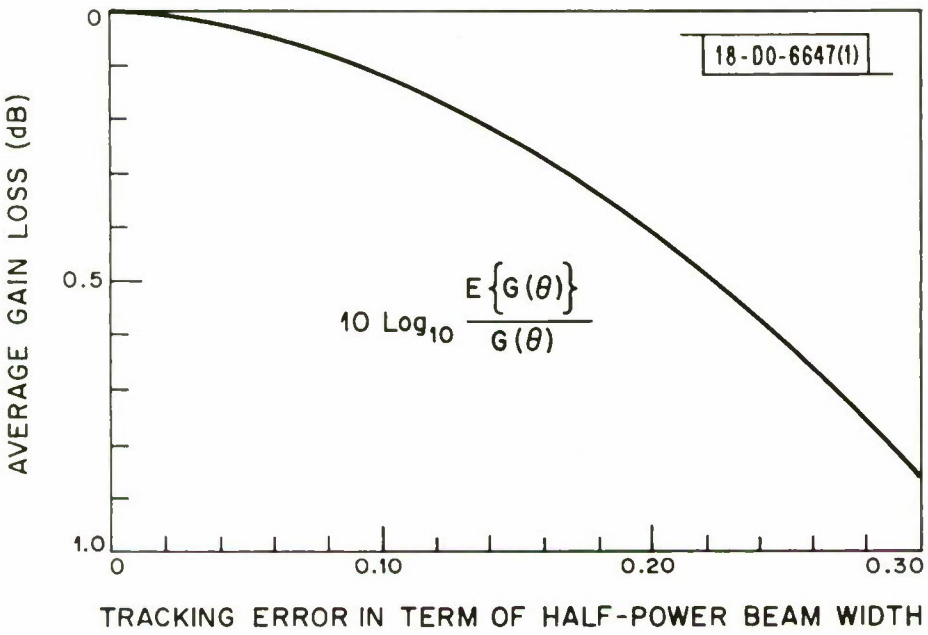

Fig. 6. Average gain loss due to tracking error.

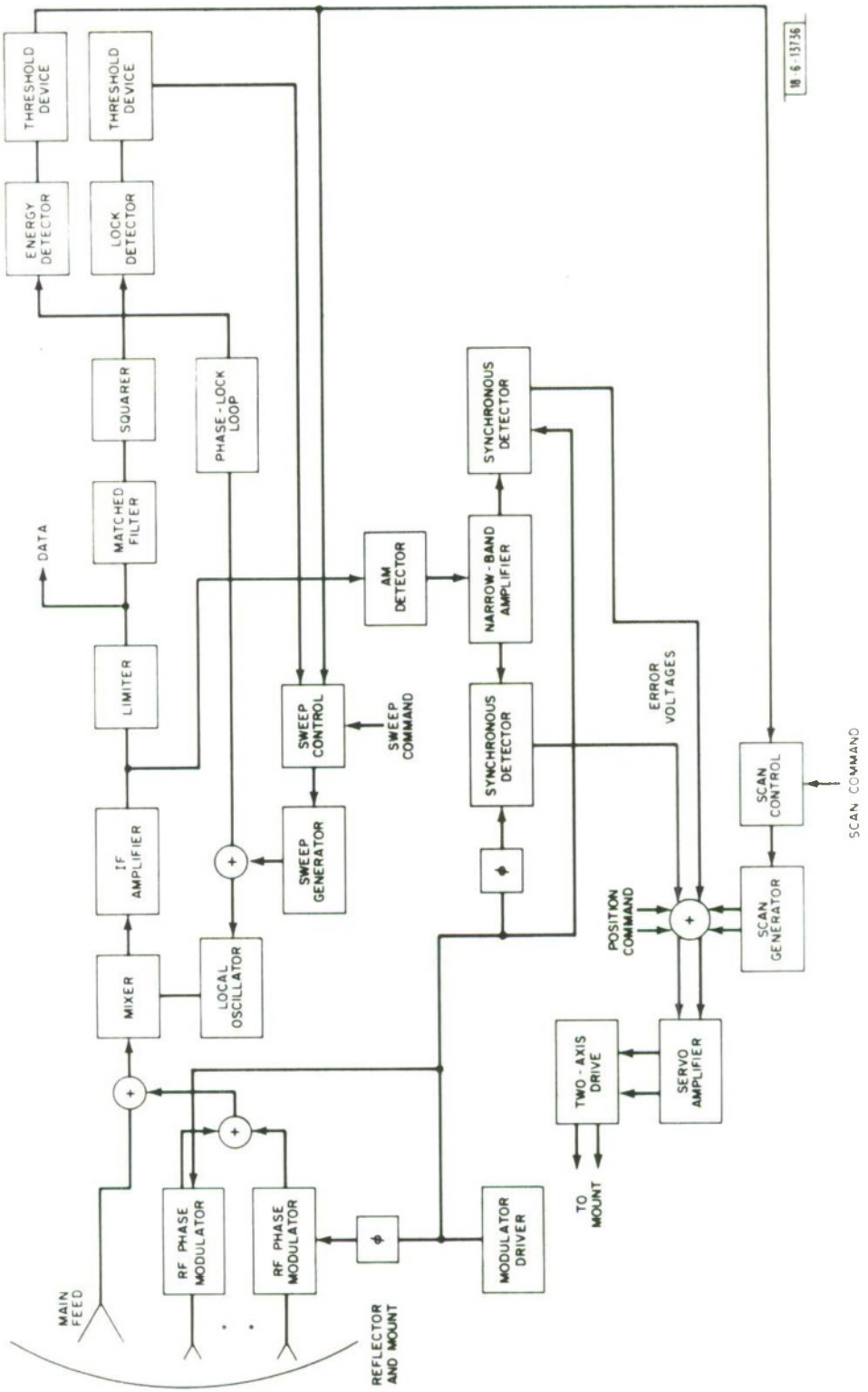

Fig. 7. Functional diagram of a single channel acquisition and tracking receiver.

channel; the tracker is efficient in utilization of power and non-selective in signal energy source. There is only one receiver channel: one mixer, and one local oscillator which is a welcome savings in equipment and in prime power in the satellite. A consequence of the single channel design is that the signal to noise power ratio is degraded by the amount of noise coupled into the sum channel and the data is contaminated by the amount of bi-phase modulated signal added to it. For a coupling factor on the order of 20 db and receiver NF $\simeq$ 9.5 db the degradation will be negligibly small. The data contamination will also be negligibly small due in part to the fact that during accurate tracking the error signal amplitude is small. The receiver bandwidth can be quite broad, the tracking function places no restrictions on it. Since the reference and the difference informations pass through the same receiver, the problems associated with differential phase and gain shifts between narrow band, high-gain channels are eliminated making this a reliable system. The beam switching is accomplished electronically not mechanically, thus the practical limit of the position tracking information capacity is quite high. Unlike with standard conical scan feeds, the transmitted signal channel operates without cross-over loss and modulation.

The method of operation is as follows. A position command is sent to each of the satellites which causes the EHF antennas to point along the line of sight. After this command is deemed to have been executed and no crosslink data is received sweep and/or scan commands are sent to each satellite so that these commands are received simultaneously. The frequency sweep is the same in each satellite, the position scan is 0.8°/sec in one satellite and sixteen times slower in the other. Because of this fairly large difference in scan speeds it will probably be adequate to initiate the search simultaneously and no special time synchronization will likely be needed. The sweep and scan generators operate until stopped through the appropriate commands or automatically through the threshold device triggered by the energy detector. The lock detector serves principally as an indicator of the status of the phase lock loop, it is also used to trigger the frequency sweep (in conjunction with the energy detector). Scan and sweep are automatically resumed when the energy detector fails to trigger the threshold device.

Because the scan pattern will overlap at the - 3 db level, once the scan generator is stopped by the energy threshold detector, the antenna is expected to align its boresight with the line of sight and track the target. The multiple beams are formed with the main and the auxiliary feeds. The outputs of these latter ones are bi-phase modulated and suitably combined, then added to the main channel. This produces a phase sensitive amplitude modulation on the composite signal. The magnitude of the modulation is proportional to the angular offset, the phase depends on the direction of the offset, and the rate is in the audio frequency range chosen by convenience and by the limitation that the Tf_B product is much larger than unity. After down conversion and amplification the modulation is recovered by the AM detector. The audio amplifier and narrow band filter further processes the signals. The outputs of the phase sensitive detectors, driven synchronously by the modulator, are the error signals which control the movements of the antenna pedestal during tracking.

SUMMARY

This note deals with the design of an acquisition and tracking system for the 55 GHz crosslink between the LES-8 and -9 satellites. Acquisition consists of scanning the spatial uncertainty of the satellites while simultaneously resolving the frequency uncertainty. Tracking implies that the narrow beam antennas are aligned along the line of sight and the carrier is centered in the bandwidth.

The LES-8, -9 satellites are intended to orbit at synchronous altitude in nearly identical non-eccentric orbits and stationkept 90° apart. Under these conditions acquisition and tracking difficulties are minimal. The crosslink parameters are influenced by the orbital parameters. Based on studies concerning crosslink parameters and their time variations, and based on current designs and previous experience, the acquisition problem is defined as scanning over a region $3^\circ \times 3^\circ$ while sweeping over a 10 kHz bandwidth. The parameters of the communication system are conservatively defined and the computed $P_r/N_o = 53.6$ db-Hz on the crosslink. This is adequate for a 10 kilobit data rate with $P_e \leq 10^{-5}$ and a margin of 4 db.

Acquisition is initiated by a pointing command followed by a sweep and/or scan command(s). The position uncertainty region is scanned in a pattern which overlaps at the half-power beamwidths. One of the antennas scans at the rate of one HPBW/sec, the other antenna scans at one-sixteenth this rate. The upper limit on the time required to cover 4 x 4 HPBW region is 256 seconds. The scanning continues until the output of the threshold detector causes the scan generator to stop. The scan overlap pattern influences the setting of the threshold level. The threshold level selected is evaluated at the - 10 db level relative to exact alignment of the antennas.

The anticipated frequency uncertainty is defined as 10 kHz. The incoming signal is a bi-phase modulated carrier without any residual carrier. The carrier is reconstructed in the receiver through a squaring process. This reduces the P_r/N_o value by approximately 10 db. The reconstructed carrier is passed through a narrow-band filter, detected, and compared in a threshold device with the preset level. Acquisition has occurred when the threshold level is exceeded. Under these circumstances the reconstructued carrier is in the narrow filter bandwidth. The sweep rate, filter bandwidth and the frequency sweep window are evaluated for various P_r/N_o values and plotted versus time required for a 90% probability of acquisition. The 10 kHz uncertainty can be searched within 0.4 sec by sweeping the oscillator at the rate of 4.6×10^4 rad/sec^2. The filter bandwidth is 50 Hz. The threshold voltage setting is 4.3 times the rms noise voltage, the false alarm probability is 10^{-4} and the average time between false alarms is 200 seconds. After acquisition the oscillator frequency is controlled by a phase lock loop tracking the reconstructed carrier. The loop bandwidth is evaluated at the design P_r/N_o for a chosen damping factor. The tracking performance, pull in time and lock-on time are also evaluated. These values appear suitable for the intended purposes.

The position tracking system employs electronic beam switching. The difference patterns are bi-phase modulated and added to the main beam causing an offset resultant beam. A phase sensitive amplitude modulation results for a target off boresight whose magnitude is proportional to the offset and whose sign indicates the direction of offset. The tracker is a single

channel system, in that respect it saves equipment and prime power; it is also a reliable and versatile system. The predicted performance is one-tenth of the HPBW rms tracking accuracy when the IF signal-to-noise power ratio is unity and the pre- and post-detection bandwidth ratio is 10^4 and the equivalent error slope is 0.2. The expected gain loss due to tracking performance is computed as 0.1 db.

The conceptual block diagram of the acquisition and tracking system is included, its salient features and method of operation are described. The system is planned to be implemented in the near future and will undergo extensive testing under dynamic conditions.

APPENDIX

The purpose of this appendix is to present a carrier acquisition and tracking scheme for a binary phase-shift keyed signal. The salient results of Refs. 1 and 2 are adapted and modified for the requirements anticipated with the LES-8 and -9 satellites.

A. Frequency Sweep

The data modulation on the crosslink is likely to be binary phase-shift keying. This will result in a signal of the form

$$\sqrt{2P_r}\, m(t) \cos \omega_c t$$

where $m(t) = \pm 1$. Since either of the two values are approximately equiprobable, the average of $m(t)$ is nearly zero and so is the carrier component of the received signal. Squaring this signal yields

$$P_r\, (1 + \cos 2\, \omega_c t)$$

which contains an unmodulated carrier component at twice the original frequency. This is a standard procedure for recreating the carrier of bi-phase modulated signals. It is our aim to acquire and track this reconstructed carrier.

The squarer is preceded with a filter in order to improve the carrier to noise power density ratio at the output. This filter is matched to one bit. At the output of the squarer we have (Ref. 2):

$$\frac{P_s}{N_s} = \frac{\frac{1}{3}\,(P_r/N_o)\,(E_b/N_o)}{1 + \frac{33}{20}\,E_b/N_o + \frac{1}{12}\left(\frac{E_b}{N_o}\right)^2}$$

From the previous link calculations we have that the $E_b/N_o = +13.6$ db when the bit rate is 10 kbps and the $P_r/N_o = +53.6$ db-Hz. Using these values, the above expression is presented graphically in Fig. 8 for the anticipated range of P_r/N_o values.

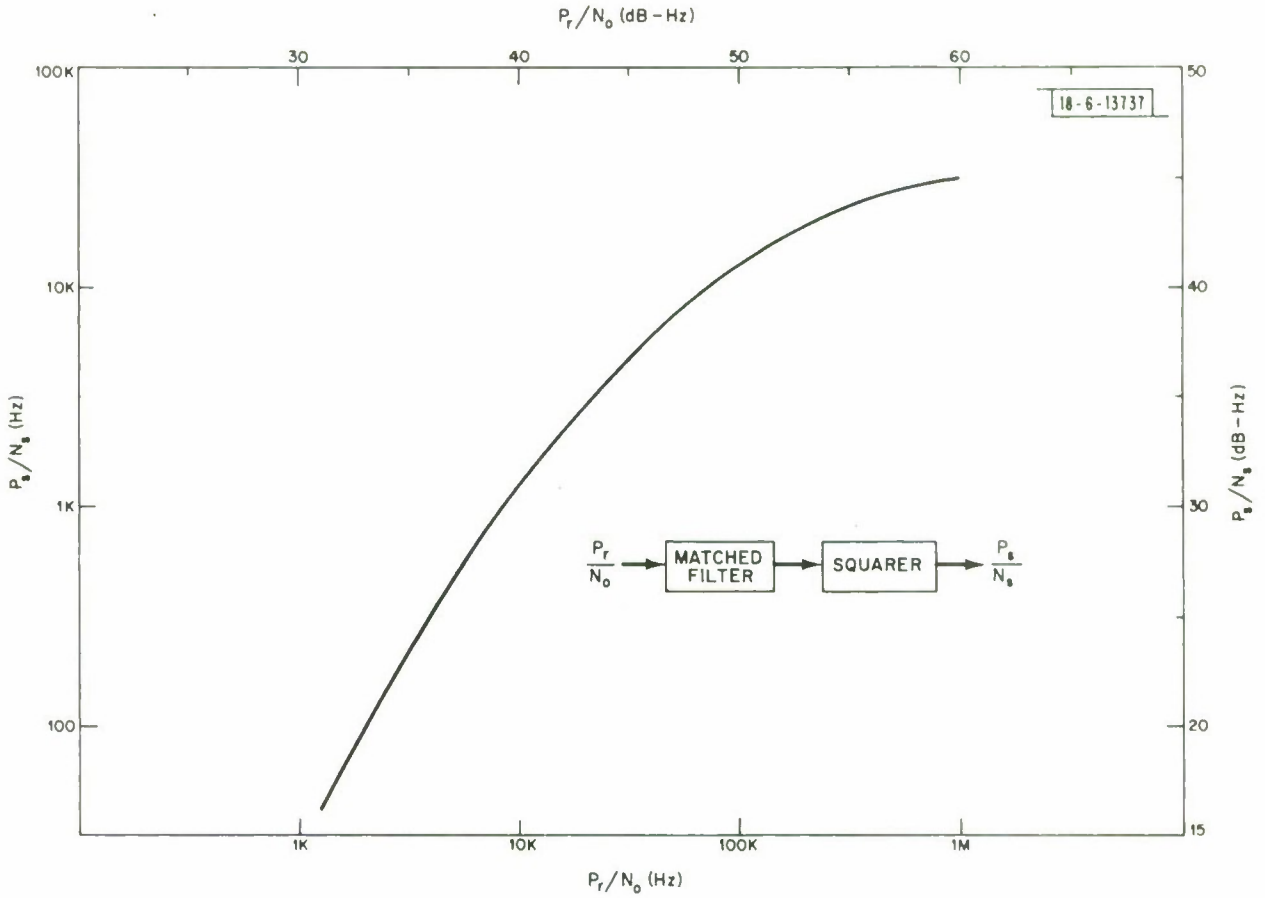

Fig. 8. Signal-to-noise power density ratio after filtering and squaring.

In addition to the desired carrier the squaring operation produces unwanted sidebands at multiples of $1/T_b$ Hz away from the reconstructed carrier, the amplitudes of the first two sidebands are -16 and -28 db relative to the amplitude of the desired line. It is possible that at high P_r/N_o's the first pair of sidebands is detected and locked onto. It will be necessary to include circuitry which can readily detect and rectify this condition.

The frequency search scheme consists of linearly sweeping the local oscillator while simultaneously monitoring the output of the narrowband energy detector. The block diagram of the frequency acquisition scheme is shown in Fig. 9. Detection occurs when the output of the square law detector exceeds the threshold power level L . This is the condition when the instantaneous angular frequency is within the filter bandwidth and the antenna beams are within a prescribed angular distance of the line of sight. The threshold device can also be triggered by noise. This false alarm probability versus threshold to noise voltage ratio is shown in Fig. 10.

The optimum sweep rate in terms of the narrower filter bandwidth W , ($W << W_1$), has been shown by Seay to be $W = \frac{1}{2}\sqrt{\frac{R}{2}}$. The average time required for frequency acquisition is directly proportional to the detection probability and the magnitude of the frequency uncertainty and inversely proportional to the sweep rate and false alarm probability. From Ref. 2:

$$\overline{T}_{ACQ} = \frac{\frac{W_A}{R}\left(\frac{1}{2} + \frac{P_M}{1-P_M}\right)}{1 - e^{-L/2\sigma^2}}$$

where

$\overline{T}_{ACQ}$ = average acquisition time

W_A = total range of frequency uncertainty to be searched

$P_M = 1 - P_D$ = probability of failure to lock on a particular sweep

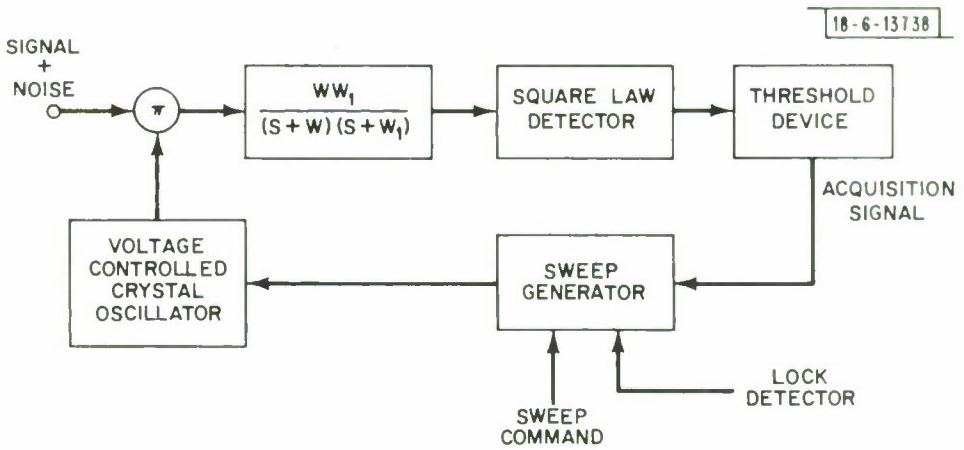

Fig. 9. Frequency acquisition scheme.

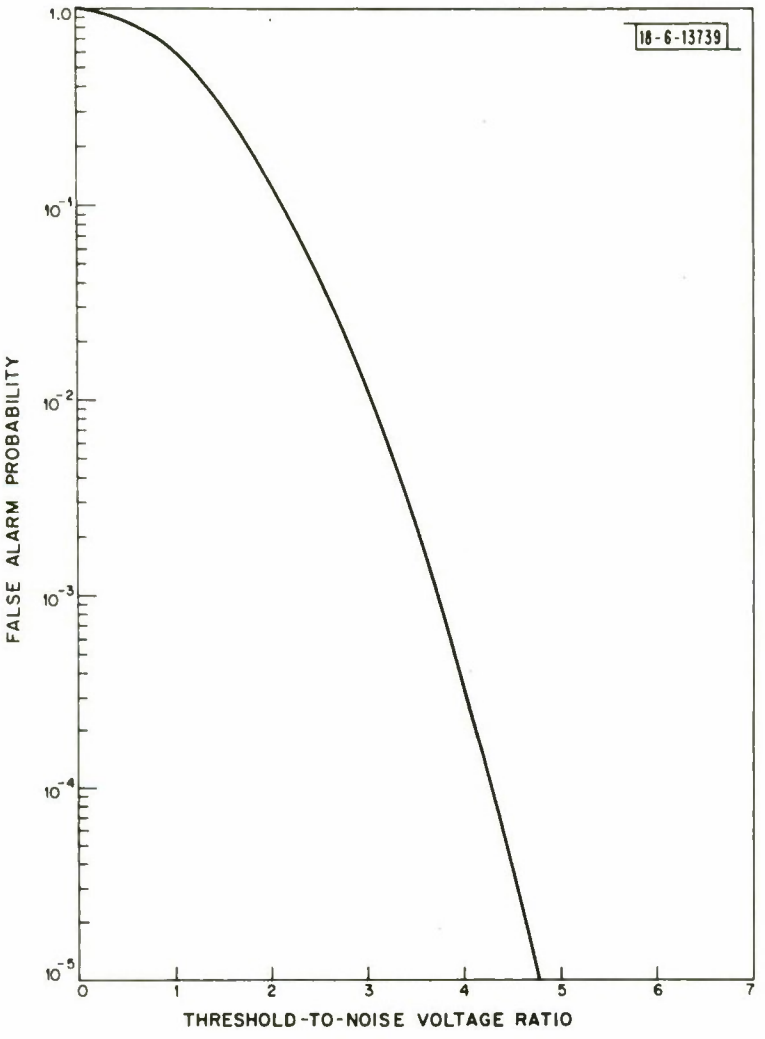

Fig. 10. False alarm probability as a function of threshold setting.

$$\sigma^2 = \frac{N_o}{2}\left(\frac{WW_1}{W+W_1}\right)$$

The average acquisition time for an arbitrarily chosen detection probability, $P_D = 0.9$, versus signal-to-noise power density ratio after the squarer, P_s/N_s, for 1, 10, 100 kHz frequency uncertainty and for various false alarm probabilities is shown in Fig. 11. The optimum sweep rate with false alarm probability as a parameter is also plotted.

Since the mechanical sweep rate is taken to be $0.8°/\text{sec} = 1$ HPBW/sec, the fast scanning antenna beam dwells in a given spatial resolution cell for 0.8 second. This is the upper limit on the time allotted for frequency sweep and acquisition unless we want to slow down the position scan. From link calculations we have $P_r/N_o = 53.6$ db-Hz. We have chosen antenna cross-over levels to be greater than or equal to -5 db relative to on-axis gain for each antenna or -10 db total for the two beams. Then the input into the squarer is 43.6 db-Hz and from Fig. 8 the output $\frac{P_s}{N_s} = 35$ db-Hz. From Fig. 11 $\overline{T}_{ACQ} = 0.4$ sec when the frequency uncertainty is 10 kHz, $P_s/N_s = 3.16 \times 10^3$ (Hz), $P_D = 0.9$ and the false alarm probability is 10^{-4}. Since the squarer acts as a frequency doubler, the actual frequency uncertainty searched is 20 kHz. Extrapolating between the curves, if we allow up to $\overline{T}_{ACQ} = 1$ sec then $W_A/2\pi = 25$ kHz or the total frequency uncertainty that can be searched in one second is 50 kHz. We note that in order to search $\frac{W_A}{2\pi} = 100$ kHz in one second the required $\frac{P_s}{N_s} = 38$ db-Hz. Selecting $\frac{P_s}{N_s} = 35$ db-Hz as the design point we see that the sweep rate $\frac{R}{2} = 4.6 \times 10^4$ rad/sec^2, again for a false alarm probability of 10^{-4}. From this sweep rate we compute $W = \frac{1}{2}\sqrt{R/2} = 107$ rad/sec. From Fig. 10 for $P_{f.a.} = 10^{-4}$ the threshold voltage setting $\frac{\sqrt{L}}{\sigma} = 4.28$. The average time between false alarms is inversely proportional to the product of bandwidth and false alarm probability. Since our narrowest bandwidth is about 50 Hz and we have

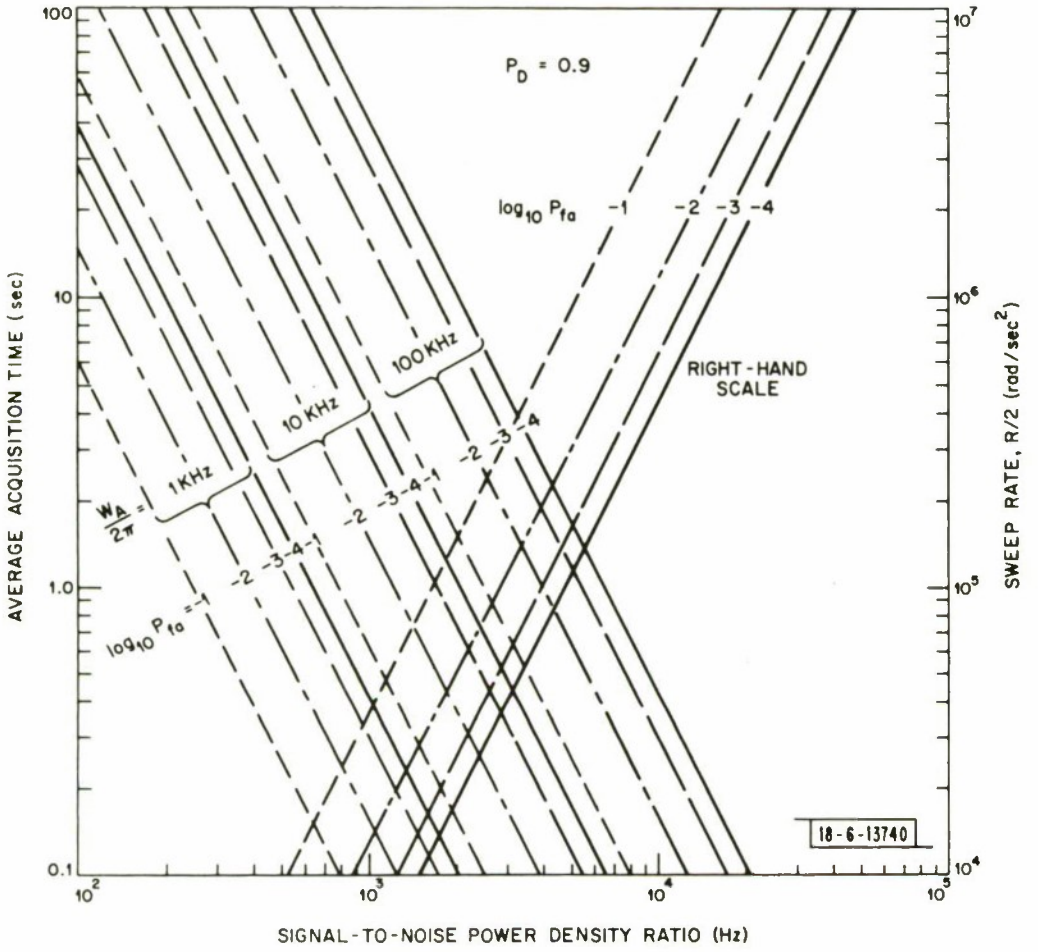

Fig. 11. Average acquisition time and sweep rate as a function of signal-to-noise ratio.

arbitrarily selected $P_{f.a.} = 10^{-4}$, $\overline{T}_{f.a.} = \frac{1}{P_{f.a.}B} = \frac{1}{(10^{-4})\ (50)} =$ 200 sec. The maximum time required to complete the position scan is 256 sec. Thus with a slightly higher threshold voltage setting we would expect the probability to be small for a false alarm to occur during acquisition.

B. Phase Lock

Because of the Doppler shift and possible oscillator drifts it will be necessary to track the incoming reconstructed carrier after acquisition. This requires a second order phase-lock loop since first order loops cannot track a frequency ramp. The design of such loops is amply treated in the literature[6]. Our purpose here is to select design parameters and estimate the expected tracking and pull in performance and to compare this with the predicted requirements.

We assume a second order loop with a damping constant $\xi = \frac{\sqrt{2}}{2}$. The relationship between the one-sided loop noise bandwidth, B_L, and the loop natural frequency, ω_n, is

$$B_L(H_z) = \left(\xi + \frac{1}{4\xi}\right)\frac{\omega_n}{2} \text{ (rad/sec)}$$

At the frequency acquisition threshold the $P_r/N_o = 43.6$ db-Hz which reduces to $P_s/N_s = 35$ db-Hz at the output of the squarer which is the input to the loop. For good loop performance at that signal level we would like the loop signal-to-noise power ratio to be + 10 db:

$$\frac{S}{N} = 10 = \frac{P_s}{N_s(2B_L)} = \frac{\text{antilog}_{10}\ 3.5\ (\text{Hz})}{2B_L}$$

from which we obtain $B_L = 158$ Hz. This is adequate to satisfy the standard requirement that $B_L << B_{IF}$ since the IF bandwidth is on the order of 10^4 Hz to accommodate the data rate. The loop natural frequency ω_n at this point is $\omega_n = 298$ radians/sec. The time rate of change of the incoming frequency, principally due to the rate of change of Doppler, causes a frequency ramp which

the loop tracks with a steady state acceleration error. Choosing this static error arbitrarily to be $5.7° = 0.1$ radian or smaller, the peak time rate of change of the reconstructed carrier, $\dot{F}$ peak, is

$$\dot{F} \text{ peak} = \frac{\omega_n^2}{2\pi} \sin (5.7°) = 1.4 \text{ kHz} \quad .$$

Because of the squaring, the incoming carrier should change slower than 700 Hz/sec for the steady-state error to remain below 0.1 radian. As can be seen from Table I, the anticipated peak Doppler rate is orders of magnitude smaller than what the phase lock loop can handle at the design point without appreciable error.

The phase-lock loop is enabled and pulls into lock after the energy detector detects the presence of the reconstructed carrier. The pull-in range is given by Gardner:

$$\Delta\omega_p = 2\sqrt{\xi\omega_n K_v} \approx 5\,\omega_n$$

where the approximation is valid for high-gain loops. The approximate pull-in range in our case is 240 Hz . The time required for the loop to pull into lock-in range is

$$t \approx \frac{(\Delta\omega)^2}{2\xi\omega_n^3}$$

which in the present case for $\Delta\omega \simeq 5\,\omega_n$ and $\xi = \sqrt{2}/2$ is 0.06 second. The lock-in range of the loop is

$$\Delta\omega_L \simeq 2\xi\omega_n = 67 \text{ Hz} \quad .$$

The lock-up transient settles in a time duration of about $\frac{1}{\omega_n}$ seconds which is 3.3 milliseconds and it is negligibly small in comparison with the time required for the loop to pull in.

In addition to the standard phase-lock loop, which is a null-seeking arrangement, another phase detector can be added. This second phase detector is driven by the same oscillator in phase quadrature. The circuitry is recognized as the synchronous AM detector: the output is proportional to the carrier amplitude and its variations. In the present case it serves the purpose of indicating the presence of the reconstructed carrier in the phase-lock loop bandwidth, i.e. it is a lock detector. The block diagram is shown in Fig. 12. The filter bandwidths should be chosen as follows (Ref. 2): $W_1 = 10\,W$ and $W = \omega_n/2 = 150$ radians/sec. The signal to noise voltage ratio $\sqrt{L}/\sigma$ for setting the threshold device should be chosen as $\frac{\sqrt{L}}{\sigma} = 4.3$ to have a false alarm probability commensurate with the previously chosen value.

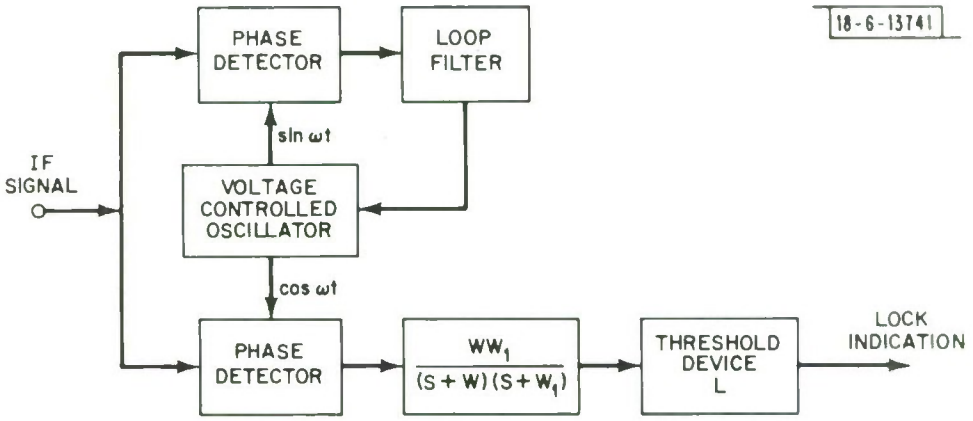

Fig. 12. Lock detection scheme.

REFERENCES

1. T. S. Seay, "A Swept Frequency Acquisition System," unpublished notes.

2. T. S. Seay and A. H. Huntoon, "A LES-5 Beacon Receiver," Technical Note 1969-27, Lincoln Laboratory, M.I.T. (1 May 1969), DDC AD-692437.

3. J. E. Tourdot, "An Analysis of a Monopulse Tracking Receiver," M.Sc. Thesis, Department of Electrical Engineering, The Ohio State University (1964).

4. L. D. Collins, private communication.

5. R. Manasse, "Maximum Angular Accuracy of Tracking a Radio Star by Lobe Comparison," IRE Trans. Antennas and Propagation, AP-8, No. 1, pp. 50-56 (January 1960).

6. F. M. Gardner, Phaselock Techniques, (J. Wiley & Sons, Inc., New York, New York, 1966).

DOCUMENT CONTROL DATA - R&D

(Security classification of title, body of abstract and indexing annotation must be entered when the overall report is classified)

1. ORIGINATING ACTIVITY *(Corporate author)*
Lincoln Laboratory, M.I.T.

2a. REPORT SECURITY CLASSIFICATION
Unclassified

2b. GROUP
None

3. REPORT TITLE
An Acquisition and Tracking Receiver for Satellite-to-Satellite Relaying at 55 GHz

4. DESCRIPTIVE NOTES *(Type of report and inclusive dates)*
Technical Note

5. AUTHOR(S) *(Last name, first name, initial)*
Zolnay, Stephen L.

6. REPORT DATE
11 May 1971

7a. TOTAL NO. OF PAGES
42

7b. NO. OF REFS
6

8a. CONTRACT OR GRANT NO. F19628-70-C-0230

b. PROJECT NO. 649L

c.

d.

9a. ORIGINATOR'S REPORT NUMBER(S)
Technical Note 1971-29

9b. OTHER REPORT NO(S) *(Any other numbers that may be assigned this report)*
ESD-TR-71-141

10. AVAILABILITY/LIMITATION NOTICES
Approved for public release; distribution unlimited.

11. SUPPLEMENTARY NOTES
None

12. SPONSORING MILITARY ACTIVITY
Air Force Systems Command, USAF

13. ABSTRACT

This note deals with the design of an acquisition and tracking system for inter-satellite communication. The problems of acquisition and tracking of position and of frequency are addressed. These are defined for the planned LES-8 and -9 satellites and a system design is proposed. The anticipated performance of the system is evaluated.

14. KEY WORDS

satellite
tracking
LES-8
LES-9